Geophysical Research Letters

RESEARCH LETTER
10.1029/2022GL099624

Large-Scale Drivers of Persistent Extreme Weather During Early Summer 2021 in Europe

A. Tuel[1], D. Steinfeld[1], S. M. Ali[1], M. Sprenger[2], and O. Martius[1,3]

[1]Institute of Geography and Oeschger Centre for Climate Change Research, University of Bern, Bern, Switzerland, [2]Institute for Atmosphere and Climate Science, ETH Zürich, Zurich, Switzerland, [3]Mobiliar Lab for Natural Risks, University of Bern, Bern, Switzerland

Key Points:

- Europe experienced unprecedented hot and wet extremes in the early summer of 2021
- Extremes resulted from recurrent blocking and wave breaking caused by a persistent meridionally amplified flow over the Atlantic
- Three extratropical transitions of hurricanes in close succession were critical in repeatedly amplifying the flow

Supporting Information:

Supporting Information may be found in the online version of this article.

Correspondence to:

A. Tuel,
alexandre.tuel@giub.unibe.ch

Citation:

Tuel, A., Steinfeld, D., Ali, S. M., Sprenger, M., & Martius, O. (2022). Large-scale drivers of persistent extreme weather during early summer 2021 in Europe. *Geophysical Research Letters*, *49*, e2022GL099624. https://doi.org/10.1029/2022GL099624

Received 17 MAY 2022
Accepted 19 SEP 2022

Author Contributions:

Conceptualization: A. Tuel, O. Martius
Data curation: A. Tuel, D. Steinfeld, S. M. Ali, M. Sprenger
Formal analysis: A. Tuel, D. Steinfeld, S. M. Ali, O. Martius
Investigation: A. Tuel, D. Steinfeld, S. M. Ali, O. Martius
Methodology: A. Tuel, D. Steinfeld, S. M. Ali, O. Martius
Resources: A. Tuel, D. Steinfeld, S. M. Ali, M. Sprenger
Software: A. Tuel, D. Steinfeld, S. M. Ali, M. Sprenger
Visualization: A. Tuel, D. Steinfeld, S. M. Ali, O. Martius
Writing – original draft: A. Tuel, D. Steinfeld, S. M. Ali, M. Sprenger, O. Martius
Writing – review & editing: A. Tuel, D. Steinfeld, S. M. Ali, M. Sprenger, O. Martius

Abstract The early summer of 2021 was a season of extremes across Europe. Heatwaves, droughts and wildfires hit Eastern Europe and the Baltic, while repeated extreme precipitation in Western Europe culminated in massive floods in mid-July. The large-scale circulation during this period was remarkably persistent, with an extremely meridionally amplified flow over Europe. Recurrent blocking over the Baltic and Rossby wave breaking in the North Atlantic led to frequent heavy precipitation in Western Europe and the Black Sea and to warm and dry conditions over Eastern Europe. These conditions persisted for a month as the blocks and wave breaking episodes strengthened one another, while three closely spaced extratropical transitions of tropical cyclones in the eastern North Atlantic led to recurrent amplification of the jet. Seasonal anomalies thus emerge from the complex interactions of individual weather events, offering an interesting storyline for climate impact assessment and a formidable challenge for (sub-) seasonal prediction.

Plain Language Summary In the early summer of 2021, Europe experienced widespread weather extremes, including record-breaking floods in Germany and prolonged heatwaves in the Baltic. These extremes resulted from a complex and particularly persistent atmospheric circulation over Europe and the North Atlantic. The interaction of three closely spaced tropical cyclones with the mid-latitude circulation led to repeated amplification of the circulation, resulting in frequent wave breaking and blocking episodes that caused the weather extremes. Understanding what led to this unusual season has important implications for current and future climate risks, and is a first step toward improving sub-seasonal forecast models to better capture such events.

1. Introduction

In the early summer of 2021 Europe experienced widespread extreme weather with significant impacts. After a very wet June, large regions of Germany, France and the Benelux experienced record accumulated precipitation in mid-July that led to devastating floods (KIT, 2021; Kreienkamp et al., 2021). The mid-July floods in Western Europe were highly damaging, claiming more than 220 lives (EM-Dat, 2021), and causing an estimated €46 billion in damages (Munich Re, 2022). Thousands of people were forced to evacuate and several communities in Germany and Belgium suffered near-total destruction. Floods occurred as well further east in Crimea in mid-June and early July following heavy precipitation (Floodlist, 2021). Several days with severe thunderstorms across the Alpine foothills and Central Europe in June also caused substantial damage (EM-Dat, 2021; ESWD, 2021). Many rivers recorded high to extreme discharge from late June to mid-July (EFAS, 2021), and by early July the levels of several Swiss lakes were approaching danger thresholds (Bundesamt für Umwelt (BAFU), 2021). Meanwhile, a large area extending from southeastern Europe to the Baltic experienced the warmest June-July since 1979 (Figure 1) and very dry conditions. These extreme conditions led to wildfires in Greece, Turkey and Italy that destroyed hundreds of thousands of hectares of forest along with dozens of homes (Reuters, 2021).

High-impact weather in Europe during summer has been connected with various weather systems. Summer heatwaves are often associated with atmospheric blocks, mainly through warm air advection, adiabatic warming due to subsidence, clear-sky radiative forcing and enhanced land-atmosphere feedbacks (Bieli et al., 2015; Drouard & Woollings, 2018; Pfahl & Wernli, 2012; Röthlisberger & Martius, 2019; Zschenderlein et al., 2019). Similarly, prolonged wet spells in Europe were related to recurrent Rossby wave breaking (RWB) (Grams et al., 2014; Mohr et al., 2020), an important precursor of heavy precipitation events (de Vries, 2021; Moore et al., 2019). RWB and blocking can also interact and maintain each other (Masato et al., 2012) through the so-called eddy-straining

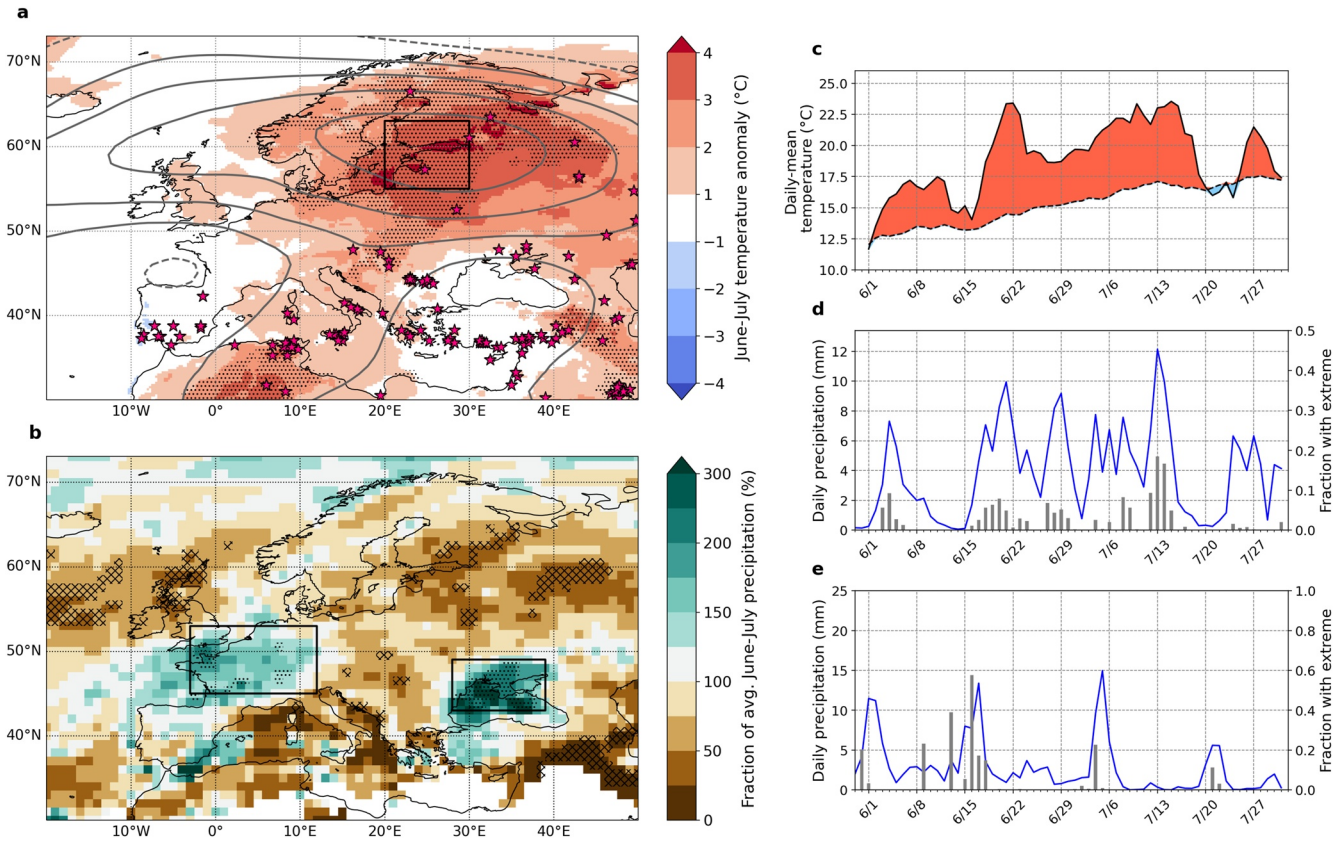

Figure 1. Extreme weather in Europe during early summer 2021. (a) ERA5 June–July 2021 averaged temperature anomaly (filled contours, C) and 500 hPa geopotential height (dashed line: −20 m; solid lines: 20–100 m at 20 m intervals) (reference: 1979–2020 June–July mean), and location of major wildfires (purple stars; events with Fire Radiation Potential ≥100 W/m^2 in VIIRS data: https://firms.modaps.eosdis.nasa.gov/download/). (b) ERA5 relative precipitation anomalies (%) with respect to the 1979–2020 June–July average. Stippling (respectively hatching) in (a, b) shows locations where anomalies were the largest to 31 July 2021, with anomalies relative to the long-term 1979–2020 mean (dashed line, C) highlighted in red (positive) and blue (negative) (d, e) ERA5 daily precipitation (blue) and fraction of area with daily precipitation above its annual 99th percentile (gray) in (d) continental Western Europe (3 W–12 E/45–53 N) and (e) the Black Sea region (28–39 E/43–49 N).

mechanism (Altenhoff et al., 2008; Hoskins et al., 1983; Shutts, 1983) while embedded precipitation and latent heat release provide further flow amplification (Lenggenhager et al., 2019; Pfahl et al., 2015; Steinfeld & Pfahl, 2019). Several periods of heavy precipitation in Europe were also caused by tropical cyclones (TCs) undergoing extratropical transition (ET) and interacting with the mid-latitude flow (Barton et al., 2016; Grams & Blumer, 2015; Grams et al., 2011). The interactions were characterized by large changes in upper-tropospheric potential vorticity (PV) due to diabatic heating and PV advection by TC outflow (Grams & Archambault, 2016), and manifest as amplified upper-level ridges and troughs. ET events are now known to be important precursors of Rossby wave initiation (Riboldi et al., 2018) and amplification (Keller et al., 2019), and high-impact weather over Europe (Pohorsky et al., 2019).

What was particularly unusual about June-July 2021, however, was the persistence of the weather for more than a month. Both hot and dry conditions in the east and wet conditions in the west lasted several weeks. Heavy to extreme precipitation fell repeatedly over Western Europe and the Black Sea between mid-June and July, resulting in record seasonal precipitation totals (Figures 1b, 1d, 1e and Figure S1 in Supporting Information S1). Similarly, in the Baltic, temperatures remained consistently above average from early June to late July (Figure 1c). The goal of this study is to identify the large-scale dynamical processes responsible for the persistent anomalous weather over Europe during early summer 2021. We specifically investigate the role of atmospheric blocking, synoptic-scale RWB and tropical-extratropical interactions in driving and maintaining the circulation in Europe. We also gain insight into the physical processes responsible for the formation of these weather systems.

2. Data and Methods

2.1. Data

The data for this study mainly come from the ERA5 reanalysis (Hersbach et al., 2020) at 0.5 spatial resolution and 6-hourly temporal resolution. We selected different variables to describe the large-scale atmospheric flow and the local-scale conditions: surface precipitation, horizontal wind, geopotential height, air temperature and relative humidity on pressure levels, and vertically integrated water vapor transport (IVT) and precipitable water. We also consider daily precipitation from the EOBS version 21.0e data set at 0.25 resolution (Cornes et al., 2018), and the Integrated Multi-satellitE Retrievals for GPM version 06 data set at 0.1 resolution (Huffman et al., 2014).

From ERA5 model-level wind, temperature, and pressure, we calculate Ertel PV which we interpolate to the 335 and 340 K isentropic levels (at which the dynamical tropopause is located during June and July (Röthlisberger et al., 2018)). As a proxy for RWB, we use PV streamers on the same two isentropic levels, which we identify with the method of Wernli and Sprenger (2007), improved by Sprenger et al. (2017). We also track blocks and upper-level ridges with the blocking detection method implemented by Steinfeld (2021) and adapted from the original index proposed by Schwierz et al. (2004). Blocks are identified as regions of persistent (70% contour overlap between consecutive six-hourly time steps for at least five days) negative anomalies of 500–150 hPa vertically integrated PV that are below the 10th percentile of the daily climatological PV anomaly distribution (1979–2020). To identify the transient ridges, we do not apply any persistent and overlap criterion. Negative PV anomalies at each time step are defined with respect to the climatological 30-day running mean (1979–2020).

Finally, we use the International Best Track Archive for Climate Stewardship data set of tropical cyclone tracks (Knapp et al., 2010). Between 15 June and 15 July 2021, three TCs developed over the North Atlantic basin and propagated northeastwards into the extratropics: TC Bill (13–16 June), TC Claudette (14–21 June) and TC Elsa (30 June–9 July).

2.2. Rossby Wave Characterization

To identify recurrent synoptic-scale Rossby wave patterns, we use the metric R (Röthlisberger et al., 2019). A 14-day running mean is first applied to six-hourly 35–65 N averaged 250 hPa meridional wind. We then filter out contributions outside the synoptic wavenumber range k = 4–15 and calculate the metric R as the absolute value of the time- and wavenumber-filtered signal.

To further analyze Rossby wave propagation, we also calculate the stationary wavenumber K^*, defined as Hoskins and Karoly (1981):

$$K^* = \cos\phi\left(\frac{\beta^*}{[u]-c}\right)^{1/2} \tag{1}$$

where ϕ is the latitude, $[u]$ the zonal wind speed and c the wave phase speed. To focus on the North Atlantic, we take $[u]$ as the 40 W-20 E sector-averaged mean zonal wind between 15 June and 15 July. β^* is the meridional gradient of absolute vorticity:

$$\beta^* = \frac{2\Omega\cos\phi}{a} - \frac{1}{a^2}\frac{\partial}{\partial\phi}\left[\frac{1}{\cos\phi}\frac{\partial}{\partial\phi}[u\cos\phi]\right] \tag{2}$$

with Ω the Earth's angular velocity and a the Earth's radius. Rossby waves are refracted toward higher values of K^*, so that a local maximum in K^* indicates a waveguide for linear wave propagation.

2.3. Backward Trajectory Calculations

To describe the dynamics of European blocks and North Atlantic ridges, we compute seven-day backward air parcel trajectories based on the three-dimensional ERA5 wind field using the Lagrangian Analysis tool LAGRANTO (Sprenger & Wernli, 2015; Wernli & Davies, 1997). Following Pfahl et al. (2015) and Steinfeld and Pfahl (2019), trajectories are started from an equidistant grid (Δx = 100 km horizontally and Δp = 50 hPa vertically between 500 and 150 hPa) within each blocking/ridge region and at each six-hourly time step, with the

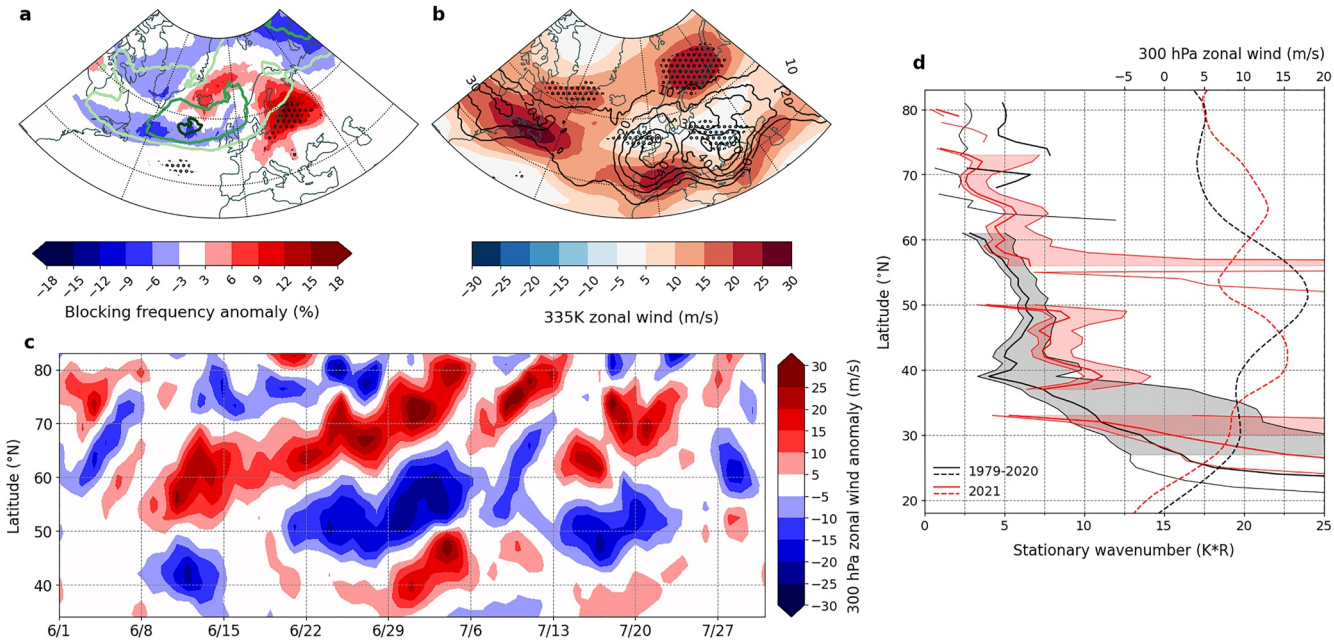

Figure 2. Anomalies of atmospheric circulation over Europe and the North Atlantic. (a) 15 June–15 July 2021 blocking frequency anomaly (filled contours), calculated with respect to the long-term 1979–2020 mean (shown by the green contours at 5%, 7.5%, and 10%). (b) 15 June–15 July 2021 mean zonal wind (filled contours) and Rossby wave breaking frequency (black contours, in %) on the 335 K level. Stippling in (a, b) indicates areas where 2021 values (of blocking frequency in (a) and zonal wind in (b)) were the highest or lowest since 1979. (c) Time series of 40 W–20 E zonal-mean zonal wind anomalies at 300 hPa from 1 June to 31 July 2021. (d) Stationary wavenumber K^* as a function of latitude, estimated from the 300 hPa 40 W–20 E zonal-mean zonal wind averaged over 1979–2020 (black lines and shading) and from 2021 values only (red lines and shading). K^* is calculated assuming a phase speed $c = 4$ m/s, with the shading showing the range when values of 1 and 9 m/s are used instead. The 300 hPa zonal wind profiles are shown by dashed lines.

additional requirement that PV must be smaller than 1 PVU to exclude parcels located in the stratosphere. We trace several variables along the trajectories (pressure, PV, potential temperature).

3. Results and Discussion

3.1. June–July 2021 Mean Circulation

We begin by describing the main features of the June–July 2021 large-scale circulation over the Euro-Atlantic region. During these two months, geopotential height anomalies show a strong high-pressure ridge centered over Finland and the Baltic States and extending across much of Northern Europe, from the British Isles to Western Russia (Figure 1a). By contrast, low-pressure troughs were located over regions to the south and on each side of the ridge (southwestern and southeastern Europe). Blocking was also much more frequent than average over the Baltic and Western Russia – blocking was present during up to 20% of all days in June and July (Figure 2a). This was far above the climatological average for the region (<5%) – it was in fact a record high frequency since 1979. Meanwhile, RWB was 2–3 times more frequent than average over Western Europe and the Black Sea (black contours on Figure 2b and Figure S2 in Supporting Information S1). The breaking waves were located on the equatorward side of the North Atlantic jet and were therefore mainly anticyclonically breaking waves (Homeyer & Bowman, 2013; Martius et al., 2007).

Another key aspect of early summer anomalies is the prevalence of a double jet pattern over the East Atlantic and Europe. Consistent with frequent blocking around the Baltic, the North Atlantic jet was split into two branches: one passing over Iceland, toward the Barents Sea, and the other across the Iberian Peninsula, merging with the subtropical jet over the Mediterranean (Figure 2b). This led upper-tropospheric zonal winds to reach record strength over Northern Scandinavia and the Barents Sea, and record lows from the British Isles to the Black Sea (Figure 2b). In some regions, the zonal wind was even directed westward and hence far from the climatological westerlies over Europe.

The double jet structure was remarkably persistent during the period, emerging during the third week of June and lasting until the last week of July (Figure 2c). Its southern branch was associated with a distinct local waveguide

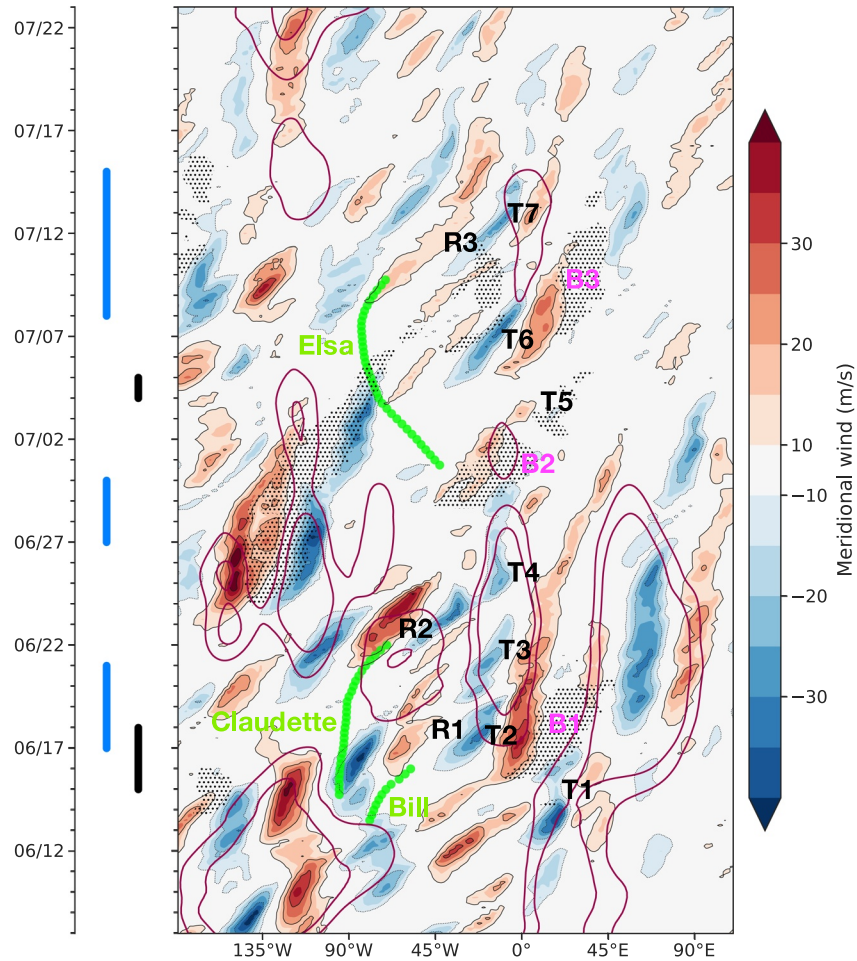

Figure 3. Hovmöller diagram for the 15 June–15 July 2021 period 35–65 N averaged meridional wind at 250 hPa (filled contours, m/s), R-metric values (purple contours at 9 and 11 m/s), longitudinal position of North Atlantic tropical cyclones (green), and longitudes at which at least half of grid points between 50 and 70 N featured an atmospheric block (stippling). Major troughs (T1–T7), North Atlantic ridges (R1–R3) and blocks (B1–B3) during this period are also indicated. Periods of extreme precipitation are shown on the left for continental Western Europe (blue) and Northern Black Sea (black).

between 35 and 50N favoring synoptic-scale disturbances (wavenumber k = 5–10; Figure 2d). The presence of this waveguide is consistent with high-amplitude recurrent Rossby waves in the Eastern North Atlantic sector between 15 June and 15 July, when the double jet was in place.

3.2. Analysis of Transient Weather Systems

A key question is to understand what set up the meridionally amplified flow in the first place, and why conditions remained so stationary during the 15 June to 15July period. The Hovmöller diagram of the meridional wind at tropopause level (250 hPa) in Figure 3 shows multiple successive ridges, troughs and blocks over the North Atlantic and Europe at approximately the same longitudes. Three separate blocks (B1–B3) occurred over the Baltic Sea and Western Russia, in mid-June, early July and mid-July, each lasting for about five days. The blocks were flanked on each side by multiple troughs that coincided with extreme precipitation in continental Western Europe or the Black Sea. To the west, troughs were split into two series, with three in close succession in the second half of June (T2–T4), and two more in the second week of July (T6–T7).

Figure 3 shows that the recurrent RWB and associated trough formation over Western Europe occurred not only upstream of blocks, but also downstream of prominent North Atlantic ridges (R1–R3) that followed the recurvature of three TCs: Bill (15 June), Claudette (21 June) and Elsa (8 July). The subsequent ridge amplification

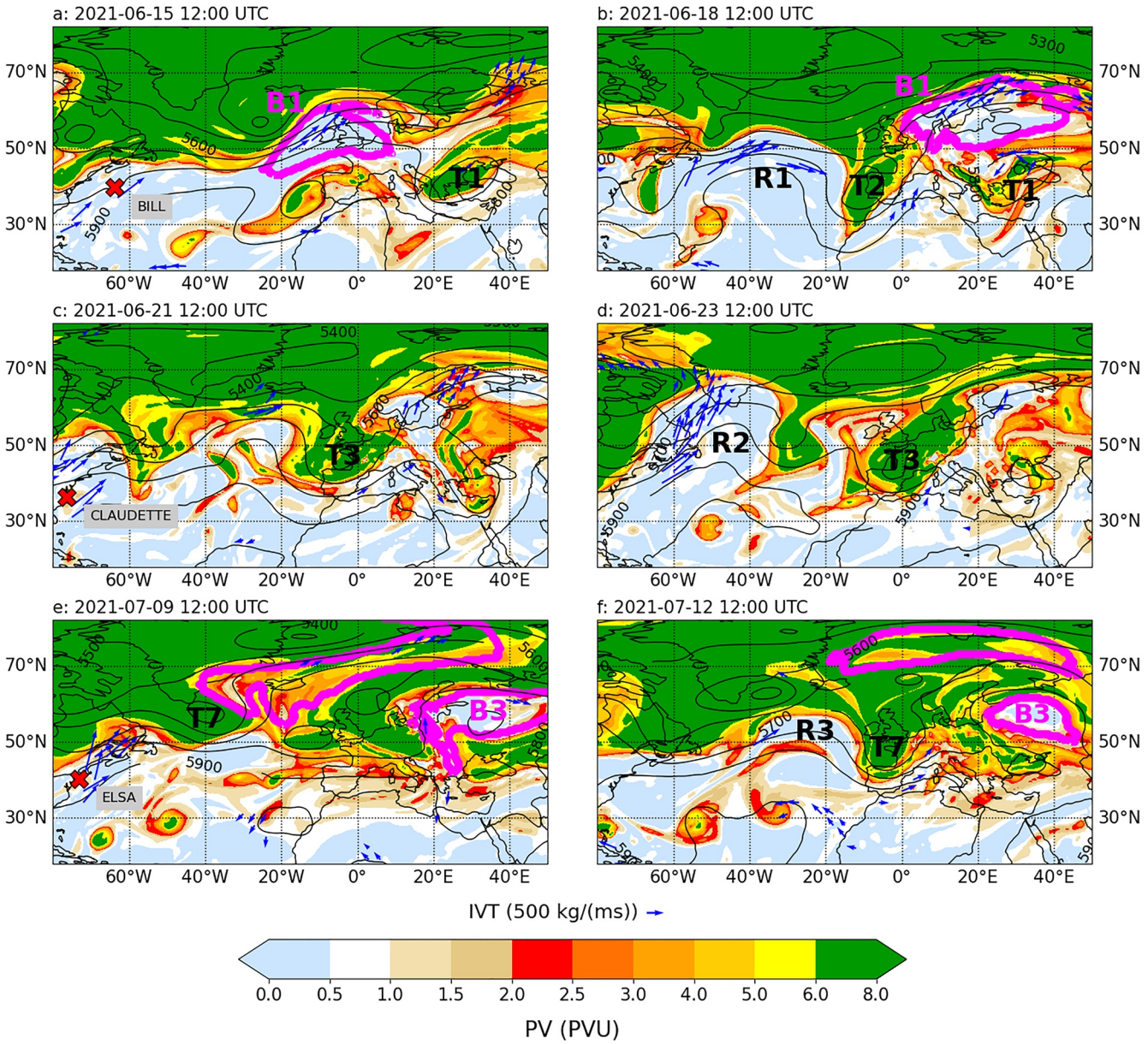

Figure 4. Isentropic potential vorticity (PV) maps at times of extratropical transitions (ETs). Maps showing PV on the 335 K level (filled contours), blocks (magenta lines), Z500 isolines (black, labeled in m) and integrated water vapour transport (only where its magnitude exceeds its 99th June/July percentile; blue arrows) at 12 UTC on various days around the ETs of (a, b) tropical cyclone (TC) Bill (c, d) TC Claudette and (e, f) TC Elsa. TC locations and names are indicated by red crosses and major synoptic features from Figure 3 are also shown.

suggests that all three TCs interacted with the mid-latitude flow, strongly distorting the jet stream and leading to recurrent Rossby waves in the eastern North Atlantic.

Further insight into the interaction between the TCs and the mid-latitude flow can be gained by looking at PV maps (Figure 4). These maps show the dynamical tropopause, which is co-located with the jet stream (transition from blue to green colors) and Rossby waves in the form of alternating high-PV troughs and low-PV ridges. All three TCs entered the mid-latitudes along the eastern North American coastline just ahead of a high-PV trough (Figure 4). Such conditions tend to favor strong interactions between TCs and the mid-latitude jet because the pre-existing low-PV ridges into which the TCs move are enhanced by polewards low-PV advection, and upper-level divergence and diabatic PV reduction associated with the TC outflow (Grams & Archambault, 2016; Keller et al., 2019). The interaction is also dependent on the speed of the TC relative to the upstream trough

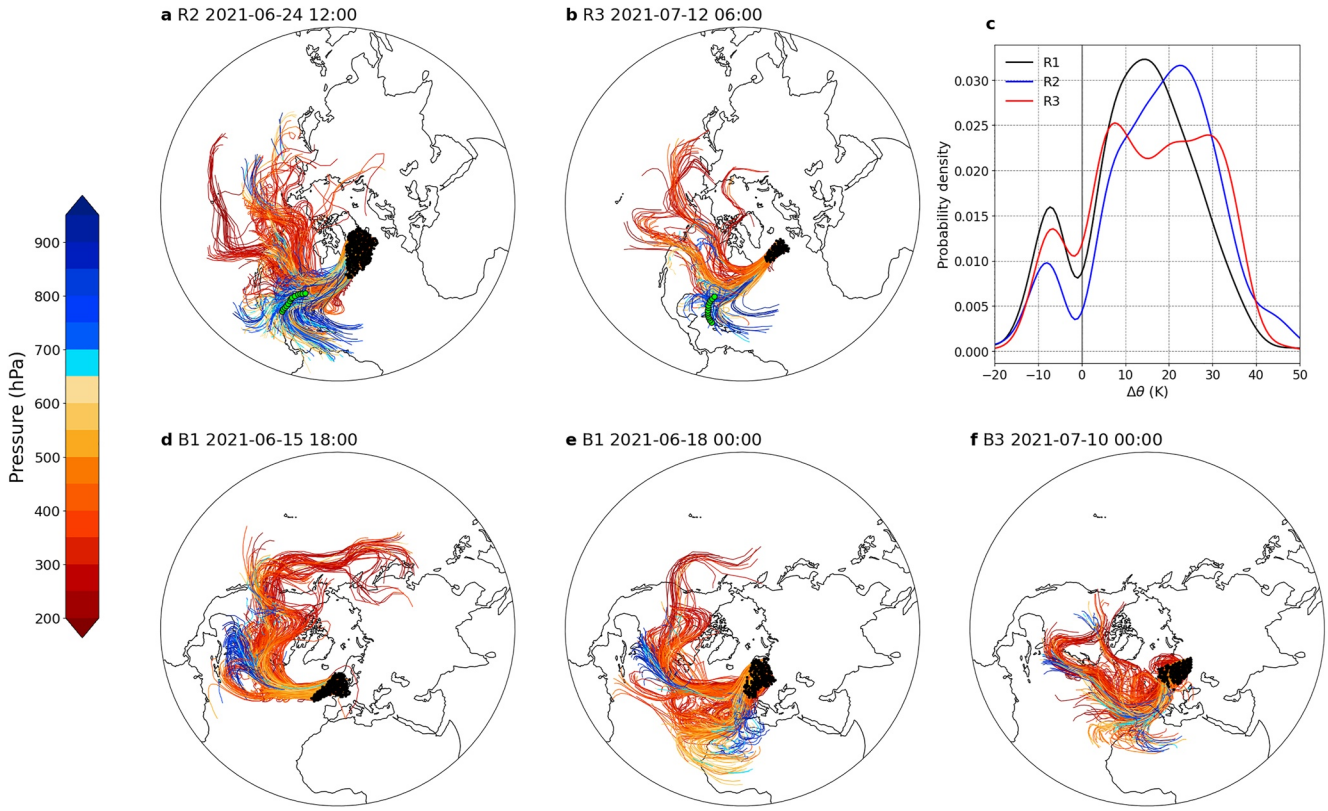

Figure 5. Backward trajectory analysis (a, b, d–f) Seven-day backward trajectories, colored according to pressure (in hPa), started from (a) ridge R2 at 12 UTC on June 24, (b) ridge R3 at 6 UTC on July 12, (d) block B1 at 18 UTC on June 15, (e) block B1 at 00 UTC on June 18, and (f) block B3 at 00 UTC on July 10. Green circles in (a–b) indicate TC positions (b: Claudette; c: Elsa) in the first three days of the trajectories. (c) Frequency distributions of maximum potential temperature (θ) change along the seven-day backward trajectories started from the three ridges.

(Brannan & Chagnon, 2020; Riboldi et al., 2019). In summer 2021, all three transitions were immediately followed by the rapid build-up of downstream ridges (R1–R3) and the subsequent meridional deformation of the dynamical tropopause and RWB over Western Europe (Figure 4). The RWB was then associated with intense vertically IVT and heavy precipitation events over Europe.

To further illustrate the connection between the transitioning TCs and the ridges, we use backward trajectories showing the pathways of air parcels ending in the ridges. The ridges evolved out of two main airstreams, a quasi-horizontal airstream confined to levels above 500 hPa and following the mid-latitude jet, and a strongly diabatically heated airstream ascending from the lower troposphere (FigureS 5a, 5b). About a third of trajectories for R2 and R3 originated from levels below 800 hPa, and about a sixth for R1. The associated air parcels experienced strong latent heating (Figure 5c) – resulting in heating maxima around ridge onset (Figure S3-a in Supporting Information S1) – and PV reduction (not shown), which contributed to the development of downstream ridges. The timing and location of the corresponding trajectories indicate that ascent took place as the TCs recurved over the Caribbean, and thus likely as part of their associated warm conveyor belts (WCBs) (Figures 5a, 5b).

Diabatic processes also played an important role for blocking onset and maintenance over Europe, consistent with recent climatological analyses (Pfahl et al., 2015; Steinfeld & Pfahl, 2019) and case studies (Croci-Maspoli & Davies, 2009; Steinfeld et al., 2020). In addition to a quasi-horizontal mid-latitude airstream, ascending airstreams originating from the Western Atlantic – not directly connected to TCs – also fed into the blocks at their onset (Figure 5d), leading to pronounced heating peaks in B1 and B2 (Figure S3-b in Supporting Information S1). Additionally, blocks B1 and B3 exhibit secondary heating maxima several days after their onset (Figure S3-b in Supporting Information S1). These maxima are associated with the development of a secondary air stream feeding into the blocks, originating from Northwestern Africa and ascending ahead of the troughs and RWB regions (thus likely as part of WCBs; Figures 5e, 5f).

In addition to ET events, the large block that developed over western North America in late June – associated with a major heatwave (Overland, 2021) – seems to have had an important influence on the North Atlantic flow (Figure 3). As it reached the North Atlantic around July 5, it distorted PV contours downstream (to the east), forming trough T6 and causing heavy precipitation in Western Europe (Figure S4 in Supporting Information S1). The remnants of this block also merged with block B3 over Western Russia, likely further adding to B3's persistence.

3.3. Atmospheric Flow Persistence From Mid-June to Mid-July

Our analysis of synoptic-scale processes shows that the persistent flow anomalies over the North Atlantic and Europe between mid-June and mid-July arose from recurrent transient systems. Three successive blocks led to unprecedented blocking frequency anomalies over the Baltic and Western Russia (Figure 2a), while Western Europe and the Black Sea experienced frequent RWB. The pattern of surface anomalies (Figures 1a, 1b) and the surface extremes emerged from this chain of events, with long-lasting warm and dry anomalies underneath the blocks and repeated heavy precipitation associated with RWB.

The persistence resulted from the repeated meridional amplification of the North Atlantic mid-latitude flow. Three ET events in close succession contributed to the amplification of the downstream flow, as well as the downstream advection of the large North American block. This makes early summer 2021 period an interesting illustration of tropical-extratropical interactions over the North Atlantic in summer that led to prolonged anomalies in the mid-latitudes (Barton et al., 2016).

The persistent meridional amplification of the flow led to frequent Rossby wave initiation and RWB, as the waves repeatedly reached their critical latitude on the equatorward side of the mid-latitude jet. At the monthly timescale, the meridional amplification translated into a double-jet configuration (Figures 2b, 2c) and a local waveguide over Western Europe, along the southern branch of the jet. This pattern was maintained by the successive blocks which likely favored eddy propagation north- and southward of the blocked areas (Shutts, 1983), and by the recurrent RWB which transferred momentum polewards (strengthening the northern jet) and enhanced the meridional PV gradients to the south due to high-PV intrusions over Europe (strengthening the southern jet and associated waveguide). The blocks and RWB episodes also strengthened one another, further enhancing the persistence. RWB over Western Europe strengthened downstream blocks (especially B1 and B3) through low-PV air advection, upper-level divergence and diabatic PV reduction following strong latent heating in rapidly ascending parcels ahead of the troughs (Figures 5e, 5f) (Lenggenhager et al., 2019; Zschenderlein et al., 2020). Conversely, blocks likely fueled RWB upstream by reducing the propagation speed of the upstream waves and creating areas of strongly diffluent flow (Altenhoff et al., 2008; Shutts, 1983).

While our analysis highlights the immediate drivers of persistent European extreme weather in summer 2021, additional mechanisms may have mattered. Sea-surface temperature anomalies or the MJO, for instance, could have affected the state of the mid-latitude jet (Barton et al., 2016; Baker et al., 2019; Di Capua et al., 2020), favoring a strong response to ET (Riboldi et al., 2019). Frequent blocking might also have been fueled by land-atmosphere feedbacks (Fischer et al., 2007).

4. Conclusion and Outlook

Persistent European weather extremes during the early summer of 2021 resulted from a complex chain of transient, synoptic-scale events, which interacted with one another and with the large-scale circulation. Blocks and RWB were unusually recurrent as a result of repeated amplification of the flow over the Atlantic. This amplification was notably driven by three closely spaced transitioning TCs. The blocks and RWB episodes also sustained each other, notably through diabatic feedbacks, and contributed to maintaining the large-scale circulation anomalies. In keeping with Rousi et al. (2022), the heatwave in Eastern Europe was associated with a double jet. Our results shed some light on causality by showing that the double jet and the heatwave both resulted from the recurrent amplification of the flow manifested by the blocks and RWB episodes.

The resulting high-impact weather was highly dependent on the specific timing and phasing of the transient systems. Had the TCs been spaced further apart, Western Europe might not have experienced such extreme recurrence of Rossby waves at the end of June. Consequently, this case study has important implications for seasonal forecasts, climate projections and attribution studies and climate risk assessment. The improved understanding of

how extreme seasonal-mean anomalies arise from the interplay between transient synoptic patterns can help better capture such episodes with seasonal prediction models. In 2021, seasonal forecasts failed to predict the extent and magnitude of observed anomalies. In fact, a warm and dry summer was expected for most of Europe below 50N (ECMWF, 2021). Seasonal forecasting in the mid-latitudes is known to be generally challenging, since internal variability linked to transient weather systems tends to dominate the influence of initial conditions and external forcing (Davies, 2015; Merryfield et al., 2020; Vitart & Robertson, 2018). Our analysis is a case in point, as the forecast models had to capture many different transient systems to correctly predict the (sub-) seasonal anomalies. Even then, ETs are known to be associated with high downstream forecast uncertainty (Keller et al., 2019), as are recurrent Rossby waves (Wirth et al., 2018) and blocks (Rodwell et al., 2013).

It is unclear whether a probability can be attributed to such a chain of events in the current or future climates. The observational record is too short to state with certainty how exceptional this chain of events was. Dealing with record-shattering events is always challenging due to observational constraints. Forecast ensembles or long climate simulations can be used to work around the problem of short records (e.g., Brunner & Slater, 2022; Kelder et al., 2022), but one can wonder whether weather or climate models are able to generate such complex chains of events along with their mutual interactions. For instance, TCs and their interaction with the mid-latitude flow occur over small spatial scales that are not well-resolved by CMIP-type climate models (Baker et al., 2022; Liu et al., 2017). Low-probability, high-impact events like those of summer 2021 might therefore be absent from counterfactual climate experiments and climate projections. This could call into question the results of detection and attribution studies of the 2021 extremes (Kreienkamp et al., 2021), and at least make us careful while interpreting them. It might be more appropriate to assign only the thermodynamical signal, since models are more trustworthy on this aspect (van Garderen et al., 2021). We also know that ET events may become more likely in the future as TCs become stronger and more frequent at higher latitudes (Studholme et al., 2022), meaning that event sequences as in 2021 could also become more frequent.

In conclusion, the early summer of 2021 offers a useful event-based storyline for climate risk assessment (Sillmann et al., 2021), and could also be used as a template to devise new storylines of high-impact weather. Additionally, this episode highlights the enormous challenges that remain in seasonal forecasting and climate modeling of extreme events.

Data Availability Statement

ERA5 reanalysis data are available from https://dx.doi.org/10.24381/cds.bd0915c6. EOBS data are available from https://doi.org/10.24381/cds.151d3ec6, and Integrated Multi-satellitE Retrievals for GPM data from https://gpm.nasa.gov/data/imerg. Code for calculating the R-metric is available at https://doi.org/10.5281/zenodo.5742810 (Ali & Röthlisberger, 2021). The blocking identification code CONTRACK is available at https://doi.org/10.5281/ZENODO.4765560 (Steinfeld, 2021).

Acknowledgments
The authors thank Heini Wernli for fruitful discussions. O.M. and S.M.A. acknowledge support from the Swiss Science Foundation Grant No. 178751. D.S. acknowledges funding from the Wyss Academy for Nature.

References

Ali, M., & Röthlisberger, M. (2021). R-metric code: Zenodo [Software]. https://doi.org/10.5281/zenodo.5742810

Altenhoff, A. M., Martius, O., Croci-Maspoli, M., Schwierz, C., & Davies, H. C. (2008). Linkage of atmospheric blocks and synoptic-scale Rossby waves: A climatological analysis. *Tellus A: Dynamic Meteorology and Oceanography*, *60*(5), 1053–1063. https://doi.org/10.1111/j.1600-0870.2008.00354.x

Baker, A. J., Roberts, M. J., Vidale, P. L., Hodges, K. I., Seddon, J., Vannière, B., et al. (2022). Extratropical transition of tropical cyclones in a multiresolution ensemble of atmosphere-only and fully coupled global climate models. *Journal of Climate*, *35*(16), 1–64. https://doi.org/10.1175/JCLI-D-21-0801.1

Baker, H. S., Woollings, T., Forest, C. E., & Allen, M. R. (2019). The linear sensitivity of the north Atlantic oscillation and eddy-driven jet to SSTs. *Journal of Climate*, *32*(19), 6491–6511. https://doi.org/10.1175/JCLI-D-19-0038.1

Barton, Y., Giannakaki, P., von Waldow, H., Chevalier, C., Pfahl, S., & Martius, O. (2016). Clustering of regional-scale extreme precipitation events in southern Switzerland. *Monthly Weather Review*, *144*(1), 347–369. https://doi.org/10.1175/MWR-D-15-0205.1

Bieli, M., Pfahl, S., & Wernli, H. (2015). A lagrangian investigation of hot and cold temperature extremes in Europe. *Quarterly Journal of the Royal Meteorological Society*, *141*(686), 98–108. https://doi.org/10.1002/qj.2339

Brannan, A. L., & Chagnon, J. M. (2020). A climatology of the extratropical flow response to recurving Atlantic tropical cyclones. *Monthly Weather Review*, *148*(2), 541–558. https://doi.org/10.1175/MWR-D-19-0216.1

Brunner, M. I., & Slater, L. J. (2022). Extreme floods in Europe: Going beyond observations using reforecast ensemble pooling. *Hydrology and Earth System Sciences*, *26*(2), 469–482. https://doi.org/10.5194/hess-26-469-2022

Bundesamt für Umwelt (BAFU). (2021). Hydrologische Daten und Vorhersagen. Retrieved from https://www.hydrodaten.admin.ch

Cornes, R. C., van der Schrier, G., van den Besselaar, E. J. M., & Jones, P. D. (2018). An ensemble version of the E-OBS temperature and precipitation data sets. *Journal of Geophysical Research: Atmospheres*, *123*(17), 9391–9409. https://doi.org/10.1029/2017JD028200

Croci-Maspoli, M., & Davies, H. C. (2009). Key dynamical features of the 2005/06 European winter. *Monthly Weather Review*, *137*(2), 664–678. https://doi.org/10.1175/2008MWR2533.1

Davies, H. C. (2015). Weather chains during the 2013/2014 winter and their significance for seasonal prediction. *Nature Geoscience*, *8*(11), 833–837. https://doi.org/10.1038/ngeo2561

de Vries, A. J. (2021). A global climatological perspective on the importance of Rossby wave breaking and intense moisture transport for extreme precipitation events. *Weather and Climate Dynamics*, *2*(1), 129–161. https://doi.org/10.5194/wcd-2-129-2021

Di Capua, G., Runge, J., Donner, R. V., van den Hurk, B., Turner, A. G., Vellore, R., et al. (2020). Dominant patterns of interaction between the tropics and mid-latitudes in boreal summer: Causal relationships and the role of timescales. *Weather and Climate Dynamics*, *1*(2), 519–539. https://doi.org/10.5194/wcd-1-519-2020

Drouard, M., & Woollings, T. (2018). Contrasting mechanisms of summer blocking over western Eurasia. *Geophysical Research Letters*, *45*(21), 12040–12048. https://doi.org/10.1029/2018GL079894

ECMWF. (2021). ECMWF charts catalogue. Retrieved from https://apps.ecmwf.int/webapps/opencharts/

EFAS. (2021). European flood awareness system (EFAS) bulletin: June-July 2021. Retrieved from https://www.efas.eu/sites/default/files/efasBulletins/2021/EFAS_Bimonthly_Bulletin_Jun_Jul2021_0.pdf

EM-Dat. (2021). EM-Dat: The international disasters database. Retrieved from https://public.emdat.be/data

ESWD. (2021). European severe weather database. Retrieved from https://eswd.eu

Fischer, E. M., Seneviratne, S. I., Lüthi, D., & Schär, C. (2007). Contribution of land-atmosphere coupling to recent European summer heat waves. *Geophysical Research Letters*, *34*(6), L06707. https://doi.org/10.1029/2006GL029068

Floodlist. (2021). Crimea-more floods after heavy rain leave 1 dead, dozens evacuated. Retrieved from https://floodlist.com/europe/crimea-floods-july-2021

Grams, C. M., & Archambault, H. M. (2016). The key role of diabatic outflow in amplifying the midlatitude flow: A representative case study of weather systems surrounding western north Pacific extratropical transition. *Monthly Weather Review*, *144*(10), 3847–3869. https://doi.org/10.1175/MWR-D-15-0419.1

Grams, C. M., Binder, H., Pfahl, S., Piaget, N., & Wernli, H. (2014). Atmospheric processes triggering the central European floods in June 2013. *Natural Hazards and Earth System Sciences*, *14*(7), 1691–1702. https://doi.org/10.5194/nhess-14-1691-2014

Grams, C. M., & Blumer, S. R. (2015). European high-impact weather caused by the downstream response to the extratropical transition of North Atlantic Hurricane Katia (2011). *Geophysical Research Letters*, *42*(20), 8738–8748. https://doi.org/10.1002/2015GL066253

Grams, C. M., Wernli, H., Böttcher, M., Čampa, J., Corsmeier, U., Jones, S. C., et al. (2011). The key role of diabatic processes in modifying the upper-tropospheric wave guide: A North Atlantic case-study. *Quarterly Journal of the Royal Meteorological Society*, *137*(661), 2174–2193. https://doi.org/10.1002/qj.891

Hersbach, H., Bell, B., Berrisford, P., Hirahara, S., Horányi, A., Muñoz-Sabater, J., et al. (2020). The ERA5 global reanalysis. *Quarterly Journal of the Royal Meteorological Society*, *146*(730), 1999–2049. https://doi.org/10.1002/qj.3803

Homeyer, C. R., & Bowman, K. P. (2013). Rossby wave breaking and transport between the tropics and extratropics above the subtropical jet. *Journal of the Atmospheric Sciences*, *70*(2), 607–626. https://doi.org/10.1175/JAS-D-12-0198.1

Hoskins, B. J., James, I. N., & White, G. H. (1983). The shape, propagation and mean-flow interaction of large-scale weather systems. *Journal of the Atmospheric Sciences*, *40*(7), 1595–1612. https://doi.org/10.1175/1520-0469(1983)040<1595:TSPAMF>2.0.CO;2

Hoskins, B. J., & Karoly, D. J. (1981). The steady linear response of a spherical atmosphere to thermal and orographic forcing. *Journal of the Atmospheric Sciences*, *38*(6), 1179–1196. https://doi.org/10.1175/1520-0469(1981)038<1179:TSLROA>2.0.CO;2

Huffman, G., Bolvin, D., Braithwaite, D., Hsu, K., Joyce, R., & Xie, P. (2014). *Integrated multi-satellitE retrievals for GPM (IMERG), version 4.4*. NASA's precipitation processing center. Retrieved from ftp://arthurhou.pps.eosdis.nasa.gov/gpmdata/. accessed 17 November, 2019.

Kelder, T., Marjoribanks, T. I., Slater, L. J., Prudhomme, C., Wilby, R. L., Wagemann, J., & Dunstone, N. (2022). An open workflow to gain insights about low-likelihood high-impact weather events from initialized predictions. *Meteorological Applications*, *29*(3), e2065. https://doi.org/10.1002/met.2065

Keller, J. H., Grams, C. M., Riemer, M., Archambault, H. M., Bosart, L., Doyle, J. D., et al. (2019). The extratropical transition of tropical cyclones. Part II: Interaction with the midlatitude flow, downstream impacts, and implications for predictability. *Monthly Weather Review*, *147*(4), 1077–1106. https://doi.org/10.1175/MWR-D-17-0329.1

KIT. (2021). Tagesrekorde - top20-Ereignisse (Temperatur, Niederschlag, Spitzenböen) an deutschen Stationen. Retrieved from http://www.wettergefahren-fruehwarnung.de/Artikel/Top20/top20.html

Knapp, K. R., Kruk, M. C., Levinson, D. H., Diamond, H. J., & Neumann, C. J. (2010). The international best track archive for climate stewardship (IBTrACS). *Bulletin of the American Meteorological Society*, *91*(3), 363–376. https://doi.org/10.1175/2009BAMS2755.1

Kreienkamp, F., Philip, S. Y., Tradowsky, J. S., Kew, S. F., Lorenz, P., Arrighi, J., et al. (2021). *Rapid attribution of heavy rainfall events leading to the severe flooding in Western Europe during July 2021 (Tech. Rep.)*. World weather attribution.

Lenggenhager, S., Croci-Maspoli, M., Brönnimann, S., & Martius, O. (2019). On the dynamical coupling between atmospheric blocks and heavy precipitation events: A discussion of the southern Alpine flood in October 2000. *Quarterly Journal of the Royal Meteorological Society*, *145*(719), 530–545. https://doi.org/10.1002/qj.3449

Liu, M., Vecchi, G. A., Smith, J. A., & Murakami, H. (2017). The present-day simulation and twenty-first-century projection of the climatology of extratropical transition in the north Atlantic. *Journal of Climate*, *30*(8), 2739–2756. https://doi.org/10.1175/JCLI-D-16-0352.1

Martius, O., Schwierz, C., & Davies, H. C. (2007). Breaking waves at the tropopause in the wintertime northern hemisphere: Climatological analyses of the orientation and the theoretical LC1/2 classification. *Journal of the Atmospheric Sciences*, *64*(7), 2576–2592. https://doi.org/10.1175/JAS3977.1

Masato, G., Hoskins, B. J., & Woollings, T. J. (2012). Wave-breaking characteristics of midlatitude blocking. *Quarterly Journal of the Royal Meteorological Society*, *138*(666), 1285–1296. https://doi.org/10.1002/qj.990

Merryfield, W. J., Baehr, J., Batté, L., Becker, E. J., Butler, A. H., Coelho, C. A. S., et al. (2020). Current and emerging developments in subseasonal to decadal prediction. *Bulletin of the American Meteorological Society*, *101*(6), E869–E896. https://doi.org/10.1175/BAMS-D-19-0037.1

Mohr, S., Wilhelm, J., Wandel, J., Kunz, M., Portmann, R., Punge, H. J., et al. (2020). The role of large-scale dynamics in an exceptional sequence of severe thunderstorms in Europe May–June 2018. *Weather and Climate Dynamics*, *1*(2), 325–348. https://doi.org/10.5194/wcd-1-325-2020

Moore, B. J., Keyser, D., & Bosart, L. F. (2019). Linkages between extreme precipitation events in the central and eastern United States and Rossby wave breaking. *Monthly Weather Review*, *147*(9), 3327–3349. https://doi.org/10.1175/MWR-D-19-0047.1

Munich Re (2022). Natural catastrophes in 2021 fact sheet (tech. Rep.). Retrieved from https://www.munichre.com/content/dam/munichre/mrwebsiteslaunches/natcat-2022/2021_Figures-of-the-year.pdf/_jcr_content/renditions/original./2021_Figures-of-the-year.pdf

Overland, J. E. (2021). Causes of the record-breaking Pacific northwest heatwave, late June 2021. *Atmosphere*, *12*(11), 1434. https://doi.org/10.3390/atmos12111434

Pfahl, S., Schwierz, C., Croci-Maspoli, M., Grams, C. M., & Wernli, H. (2015). Importance of latent heat release in ascending air streams for atmospheric blocking. *Nature Geoscience*, *8*(8), 610–614. https://doi.org/10.1038/ngeo2487

Pfahl, S., & Wernli, H. (2012). Quantifying the relevance of atmospheric blocking for co-located temperature extremes in the Northern Hemisphere on (sub-)daily time scales. *Geophysical Research Letters*, *39*(12). https://doi.org/10.1029/2012GL052261

Pohorsky, R., Röthlisberger, M., Grams, C. M., Riboldi, J., & Martius, O. (2019). The climatological impact of recurving north Atlantic tropical cyclones on downstream extreme precipitation events. *Monthly Weather Review*, *147*(5), 1513–1532. https://doi.org/10.1175/MWR-D-18-0195.1

Reuters (2021). Southern Europe battles wildfires as north cleans up after floods. Retrieved from https://www.reuters.com/world/europe/southern-europe-battles-wildfires-north-cleans-up-after-floods-2021-07-26/

Riboldi, J., Grams, C. M., Riemer, M., & Archambault, H. M. (2019). A phase locking perspective on Rossby wave amplification and atmospheric blocking downstream of recurving western north Pacific tropical cyclones. *Monthly Weather Review*, *147*(2), 567–589. https://doi.org/10.1175/MWR-D-18-0271.1

Riboldi, J., Röthlisberger, M., & Grams, C. M. (2018). Rossby wave initiation by recurving tropical cyclones in the western north Pacific. *Monthly Weather Review*, *146*(5), 1283–1301. https://doi.org/10.1175/MWR-D-17-0219.1

Rodwell, M. J., Magnusson, L., Bauer, P., Bechtold, P., Bonavita, M., Cardinali, C., et al. (2013). Characteristics of occasional poor medium-range weather forecasts for Europe. *Bulletin of the American Meteorological Society*, *94*(9), 1393–1405. https://doi.org/10.1175/BAMS-D-12-00099.1

Röthlisberger, M., Frossard, L., Bosart, L. F., Keyser, D., & Martius, O. (2019). Recurrent synoptic-scale Rossby wave patterns and their effect on the persistence of cold and hot spells. *Journal of Climate*, *32*(11), 3207–3226. https://doi.org/10.1175/JCLI-D-18-0664.1

Röthlisberger, M., & Martius, O. (2019). Quantifying the local effect of northern hemisphere atmospheric blocks on the persistence of summer hot and dry spells. *Geophysical Research Letters*, *46*(16), 10101–10111. https://doi.org/10.1029/2019GL083745

Röthlisberger, M., Martius, O., & Wernli, H. (2018). Northern hemisphere Rossby wave initiation events on the extratropical jet?A climatological analysis. *Journal of Climate*, *31*(2), 743–760. https://doi.org/10.1175/JCLI-D-17-0346.1

Rousi, E., Kornhuber, K., Beobide-Arsuaga, G., Luo, F., & Coumou, D. (2022). Accelerated western European heatwave trends linked to more-persistent double jets over Eurasia. *Nature Communications*, *13*, 3851. https://doi.org/10.1038/s41467-022-31432-y

Schwierz, C., Croci-Maspoli, M., & Davies, H. C. (2004). Perspicacious indicators of atmospheric blocking. *Geophysical Research Letters*, *31*(6), L06125. https://doi.org/10.1029/2003GL019341

Shutts, G. J. (1983). The propagation of eddies in diffluent jetstreams: Eddy vorticity forcing of 'blocking' Flow fields. *Quarterly Journal of the Royal Meteorological Society*, *109*(462), 737–761. https://doi.org/10.1002/qj.49710946204

Sillmann, J., Shepherd, T. G., van den Hurk, B., Hazeleger, W., Martius, O., Slingo, J., & Zscheischler, J. (2021). Event-based storylines to address climate risk. *Earth's Future*, *9*(2), e2020EF001783. https://doi.org/10.1029/2020EF001783

Sprenger, M., Fragkoulidis, G., Binder, H., Croci-Maspoli, M., Graf, P., Grams, C. M., et al. (2017). Global climatologies of Eulerian and Lagrangian flow features based on ERA-interim. *Bulletin of the American Meteorological Society*, *98*(8), 1739–1748. https://doi.org/10.1175/BAMS-D-15-00299.1

Sprenger, M., & Wernli, H. (2015). The LAGRANTO Lagrangian analysis tool-Version 2.0. *Geoscientific Model Development*, *8*(8), 2569–2586. https://doi.org/10.5194/gmd-8-2569-2015

Steinfeld, D. (2021). ConTrack - contour tracking of circulation anomalies in weather and climate data. [Software]. https://doi.org/10.5281/ZENODO.4765560

Steinfeld, D., Boettcher, M., Forbes, R., & Pfahl, S. (2020). The sensitivity of atmospheric blocking to upstream latent heating – Numerical experiments. *Weather and Climate Dynamics*, *1*(2), 405–426. https://doi.org/10.5194/wcd-1-405-2020

Steinfeld, D., & Pfahl, S. (2019). The role of latent heating in atmospheric blocking dynamics: A global climatology. *Climate Dynamics*, *53*(9), 6159–6180. https://doi.org/10.1007/s00382-019-04919-6

Studholme, J., Fedorov, A. V., Gulev, S. K., Emanuel, K., & Hodges, K. (2022). Poleward expansion of tropical cyclone latitudes in warming climates. *Nature Geoscience*, *15*(1), 14–28. https://doi.org/10.1038/s41561-021-00859-1

van Garderen, L., Feser, F., & Shepherd, T. G. (2021). A methodology for attributing the role of climate change in extreme events: A global spectrally nudged storyline. *Natural Hazards and Earth System Sciences*, *21*(1), 171–186. https://doi.org/10.5194/nhess-21-171-2021

Vitart, F., & Robertson, A. W. (2018). The sub-seasonal to seasonal prediction project (S2S) and the prediction of extreme events. *npj Climate and Atmospheric Science*, *1*, 3. https://doi.org/10.1038/s41612-018-0013-0

Wernli, H., & Davies, H. C. (1997). A Lagrangian?based analysis of extratropical cyclones. I: The method and some applications. *Quarterly Journal of the Royal Meteorological Society*, *123*(538), 467–489. https://doi.org/10.1002/qj.49712353811

Wernli, H., & Sprenger, M. (2007). Identification and ERA-15 climatology of potential vorticity streamers and cutoffs near the extratropical tropopause. *Journal of the Atmospheric Sciences*, *64*(5), 1569–1586. https://doi.org/10.1175/JAS3912.1

Wirth, V., Riemer, M., Chang, E. K. M., & Martius, O. (2018). Rossby wave packets on the midlatitude waveguide?a review. *Monthly Weather Review*, *146*(7), 1965–2001. https://doi.org/10.1175/MWR-D-16-0483.1

Zschenderlein, P., Fink, A. H., Pfahl, S., & Wernli, H. (2019). Processes determining heat waves across different European climates. *Quarterly Journal of the Royal Meteorological Society*, *145*(724), 2973–2989. https://doi.org/10.1002/qj.3599

Zschenderlein, P., Pfahl, S., Wernli, H., & Fink, A. H. (2020). A Lagrangian analysis of upper-tropospheric anticyclones associated with heat waves in Europe. *Weather and Climate Dynamics*, *1*(1), 191–206. https://doi.org/10.5194/wcd-1-191-2020